Laser calibration system and lost muons correction in the g-2 experiment

Maria Domenica Galati
Università di Pisa

Supervisors: Marco Incagli, Anna Driutti

Abstract

The Muon g-2 experiment at Fermilab has the main goal to measure the muon anomalous magnetic moment $a_\mu = (g-2)/2$ to a precision of 0.14 parts per million (ppm), which means 4 times improvement in precision with respect to the final result from BNL:

$$a_\mu\,(\text{expt. BNL}) = 11659208.0(6.3) \times 10^{-10} \quad (0.54\ \text{ppm})$$

In this report I summarize the work done at the g-2 experiment during my summer internship at Fermilab. In the first two weeks my first task has been to replace the NIM logic used in the Laser Calibration System with a new FPGA. Then, I was involved in the Lost Muons analysis studying both real data and MonteCarlo simulations.

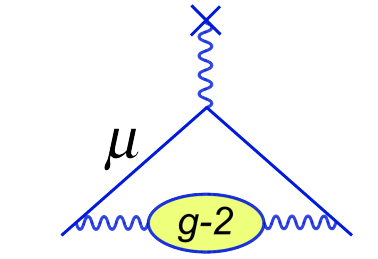

Fermilab

1. Overview and principles of g-2 measurements

1.1. Lepton Magnetic Moments

According to the Dirac theory, an electron or a muon is a pointlike particle that possesses a magnetic moment equal to:

$$\mu = \frac{e\hbar}{2mc} \tag{1}$$

where m is the lepton mass. Generally, the magnetic moment μ is related to the spin vector $\mathbf{s}$ by

$$\boldsymbol{\mu} = g\mu\boldsymbol{s} \tag{2}$$

where g is the so-called Landé g-factor. The Dirac theory predicts for particles of spin-$\frac{1}{2}$:

$$g = 2 \tag{3}$$

but small deviations from this value arise from riadiative corrections to the Dirac moment (contributions from quantum electrodynamics, electroweak theory, QCD) [1]. This additional contribute is normally written in terms of the *anomalous magnetic moment* $a = \frac{g-2}{2}$ as:

$$\mu = (1+a)\frac{e\hbar}{2m} \tag{4}$$

The anomaly a was first predicted to be $a = \frac{\alpha}{2\pi}$ for all leptons by Schwinger in 1948. Higher order terms are different for electrons, muons and taus because of their different masses.

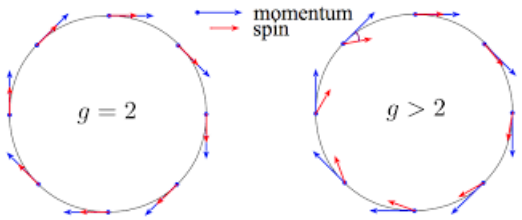

Figure 1: *Momentum and spin direction if g=2 and if g>2.*

1.2. The experiment

The currently most precise measurement of the muon anomaly a_μ was performed by the Brookhaven experiment E821. It shows a 3.6 standard deviation discrepancy from the Standard Model. The new g-2 experiment at Fermilab will measure a_μ with a factor of 4 improved precision by collecting $\simeq 20$ times the BNL statistics and improving the systematic uncertainty, thus with the possibility of increasing the discrepancy between the measured and theoretical values to 7.5σ, if the central value remains unchanged [2].

1.2. Experimental Technique

Polarized muons, produced naturally from pion decay, are injected into a 15 m diameter superconductive magnetic storage ring, that produces a magnetic dipole field $|\vec{B}| \simeq 1.45$ T.

Assuming a perfect vertical magnetic field, with a muon on the ideal orbit, the anomalous precession frequency $\vec{\omega}_a$ is defined as the difference between the spin frequency $\vec{\omega}_s$ and the cyclotron frequency $\vec{\omega}_c$ (Eq. 5).

$$\vec{\omega}_s = \frac{e\,\vec{B}}{m\gamma}(1 + \gamma a_\mu) \qquad \vec{\omega}_c = \frac{e\,\vec{B}}{m\gamma} \tag{5}$$

In absence of any other external field:

$$\vec{\omega}_a = \frac{e}{m} a_\mu \vec{B} \tag{6}$$

Electrostatic quadrupoles are used to confine the muon beam in the storage region and to provide vertical focusing. The application of an electric field introduces a new term to Equation 6, where relativistic particles feel a motional magnetic field proportional to $\vec{\beta} \times \vec{E}$. Here, $\vec{\beta}$ denotes the muon velocity and $\vec{E}$ is the electric field.
In full, the equation for $\vec{\omega}_a$ is

$$\vec{\omega}_a = \frac{e}{mc}\left[a_\mu \vec{B} - \left(a_\mu - \frac{1}{\gamma^2 - 1}\right)\vec{\beta} \times \vec{E} - a_\mu \left(\frac{\gamma}{\gamma + 1}\right)(\vec{\beta} \cdot \vec{B})\,\vec{\beta}\right] \tag{7}$$

where the third term additionally accounts for those muons whose motion is not perpendicular to the magnetic field.
The ω_a measurement is performed at a *"magic momentum"* of $\gamma = 29.3$, so that the second term in Eq. 7 vanishes. The majority of off-momentum muons are removed using collimators. However, a small momentum spread of remaining muons away from the magic momentum persists and some also experience a small amount of vertical pitching. These effects correspond to the second and third terms of equation 7 respectively. The magnitudes of these effects are determined using data, allowing for well-known, sub-parts-per-million systematic corrections and corresponding uncertainties to be applied to the measured ω_a [3].

A muon having the magic momentum will decay with a mean life-time $\gamma\tau_0 \simeq 64$ μs via a three body weak decay: $\mu^+ \to e^+ \nu_e \bar{\nu}_\mu$.
Since the decay proceeds through the weak force, it is parity violating. As a consequence, a left-handed neutrino ν_{eL} and a right-handed anti-neutrino $\bar{\nu}_{\mu R}$ are produced. The positron will be right-handed like the muon, thus preferably emitted in the same direction of the muon spin. Therefore, the ω_a can be measured fitting the rate of the more energetic positrons with the following 5 parameters formula:

$$N(t) = N_0 e^{-t/\tau}\left[1 - A\cos(\omega_a t + \varphi)\right] \tag{8}$$

where the energy and the decay time of the positrons are measured using 24 calorimeter stations located along the ring.

Finally, to have a measurement of a_μ, it is sufficient to precisely measure ω_a and $\vec{B}$.

1.3. Laser Calibration System

To precisely measure the energy and time of the positrons, all the 24 calorimeters need to be calibrated. Calibration is achieved using a laser system, which monitors the gain fluctuations, ensures performance stability of the detectors throughout long data taking periods, time-synchronizes all detectors and can also emulate the signals coming from muon decays. The laser calibration pulses are generated by 6 identical lasers, each one serving 4 calorimeters.
The Laser Control Board (LCB) manages the interface between the beam cycle and the calibration system itself. It takes care of the generation of the laser pulses and distributes the time reference signals to the monitoring electronics [6].

The laser calibration system is used in two operating modes: *Standard operation mode* and *Double-pulse mode*.

- in the *Standard operation mode* a regular pattern of laser pulses is sent and used offline to calibrate the calorimeters (Figure 2)

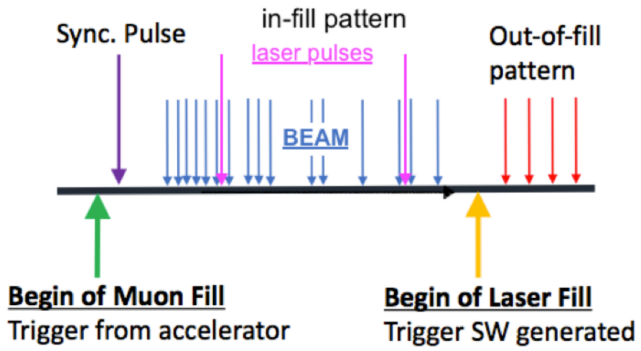

Figure 2: *Standard operation mode: laser pulses are sent at the beginning, during and after the muon fill.*

- in the *Double-pulse mode* two consecutive laser pulses are sent to all crystals with a delay that can vary up to several hundreds of μs. The goal is to measure the calorimeter gain drop when two or more particles hit the same crystal.
  There are two implementations of the *Double-pulse mode*:
  - *Short Term Double Pulse*: the second pulse is delayed by $0 \div 80$ ns with respect to the first (Figure 3)
  - *Long Time Double Pulse*: a test pulse is sent with a delay of $0 \div 60$ μs from a burst of pulses mimicking the initial splash of the incoming beam (Figure 4).

To monitor the laser intensity event-by-event, special detectors called *Source Monitors* are used. Each Source Monitor consists of (Figure 5):

- two PIN diodes, used to monitor the intensity of the laser pulses (*fast monitoring*);
- one PMT with an Americium source embedded, used as an absolute monitor (*slow absolute monitoring*).

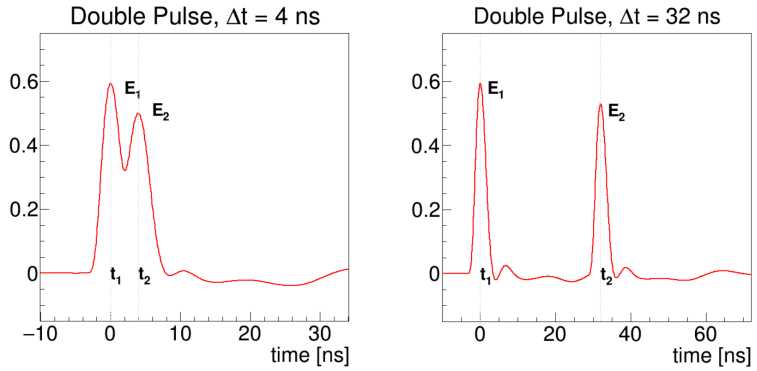

Figure 3: *Short Term Double Pulse schematic structure.*

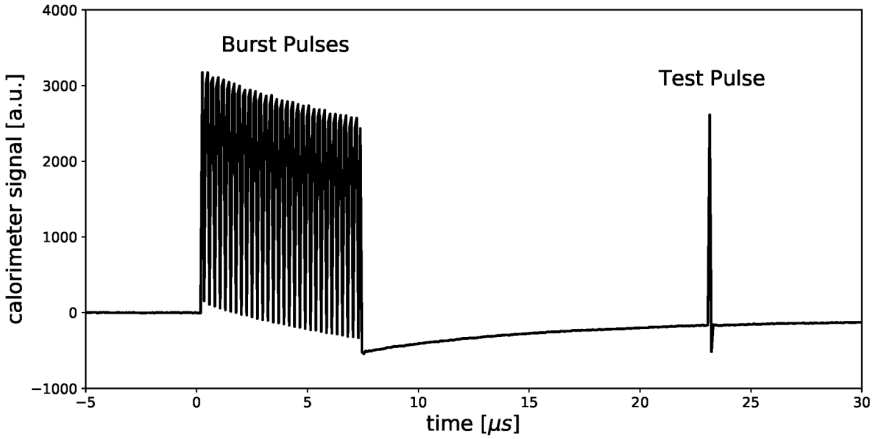

Figure 4: *Long Term Double Pulse schematic structure.*

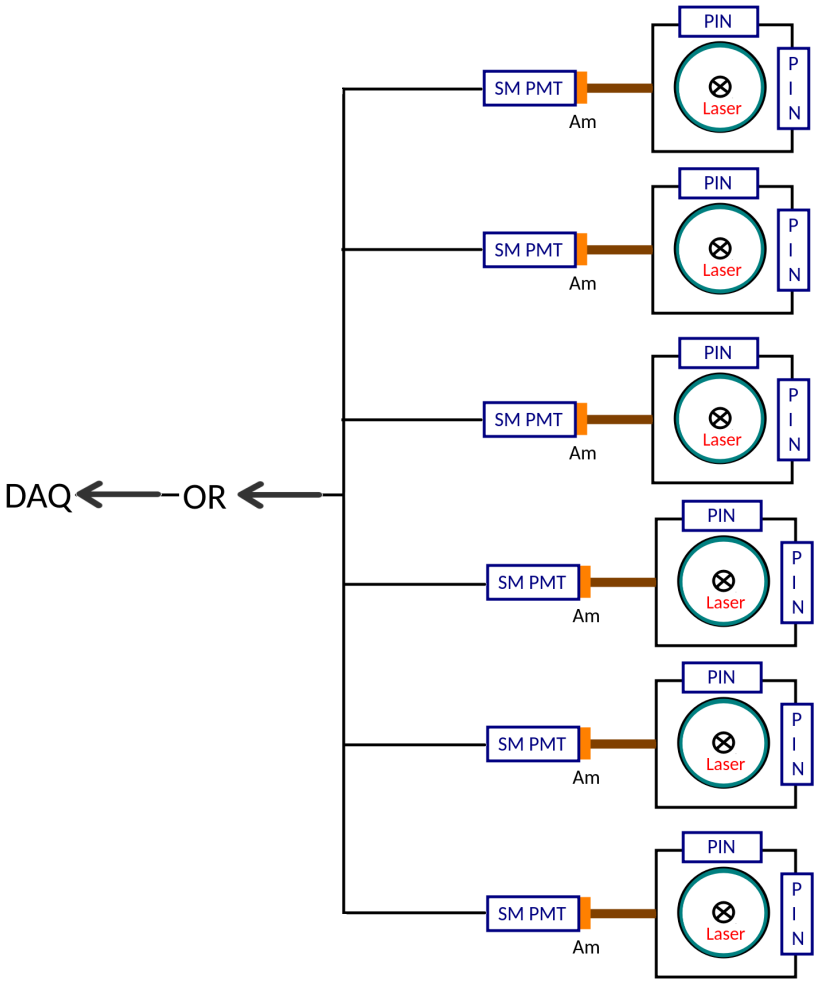

Figure 5: *Schematic structure of Source Monitors*

2. Reorganization of the trigger logic

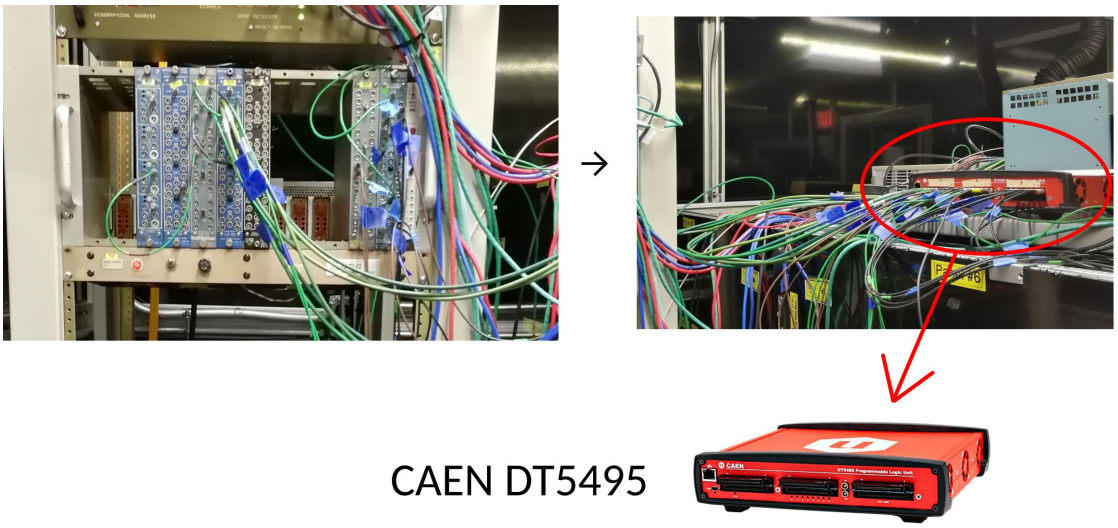

Figure 6: *Left: NIM logic (old). Right: FPGA logic (new).*

Up to the end of July 2019, both the Americium and the laser triggers were handled by NIM logic. My first task has been to replace it with FPGA logic (Fig. 6).

The input signals coming from the Laser Control Board, the Short Term and Long Term Double Pulse are grouped into two categories, EVEN and ODD, depending on which of the 6 lasers they belong.
The output signals providing the laser trigger are: (3x) Logic OR of all EVEN signals, (3x) Logic OR of all ODD signals, while the output signals from the SMs are: (2x) Logic OR of all the SM signals, Logic OR of 1, 2, 3 SM signals and Logic OR of 4, 5, 6 SM signals.
The Programmable Logic Unit `CAEN DT5495` has been programmed with Sci-Compiler as shown in Figure 7. The setup is shown in Figure 8.

The amplitude of the TTL output signal was measured to be less than 1.8 V, as shown in Figure 10a. This was an issue since 1.8 V was lower the 3.3 V threshold required by the acquisition system. After disassembling the `DT5495` I found a set of jumpers corresponding to the output signal impedences. Moving their position to 50Ω termination, as shown in Figure 9, fixed the amplitude to standard TTL (Figure 10b).
The Sci-Compiler code in Fig. 7 was finally uploaded to the FPGA, that is now routinely working in the Laser Hut.

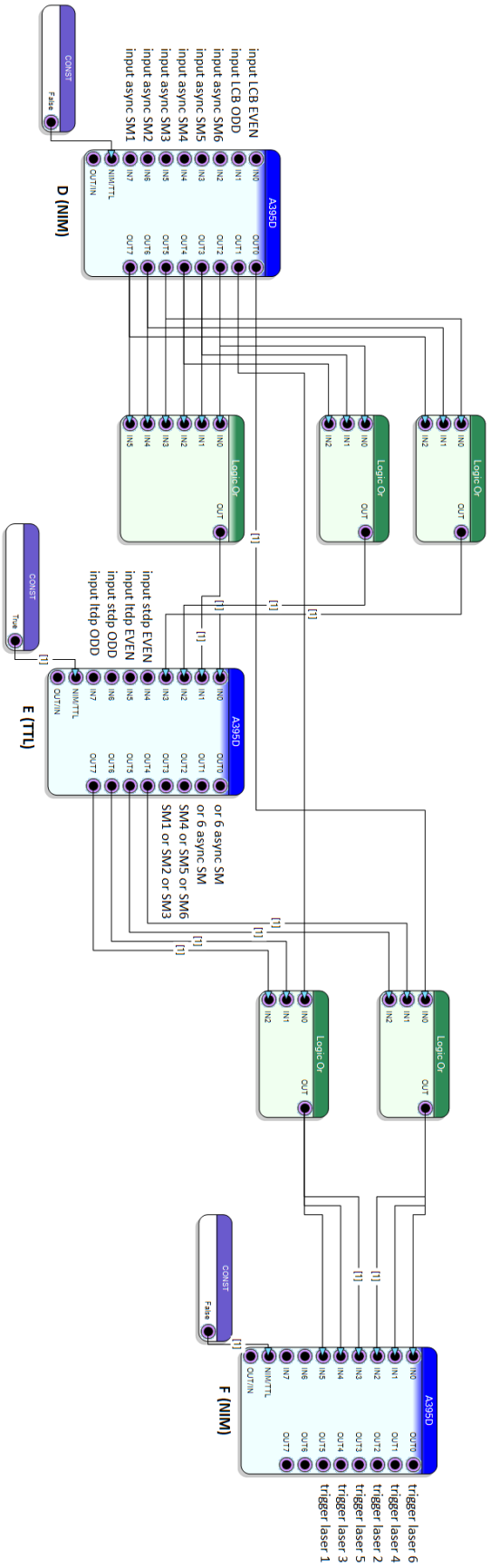

Figure 7: *Code used to update firmware of the FPGA.*

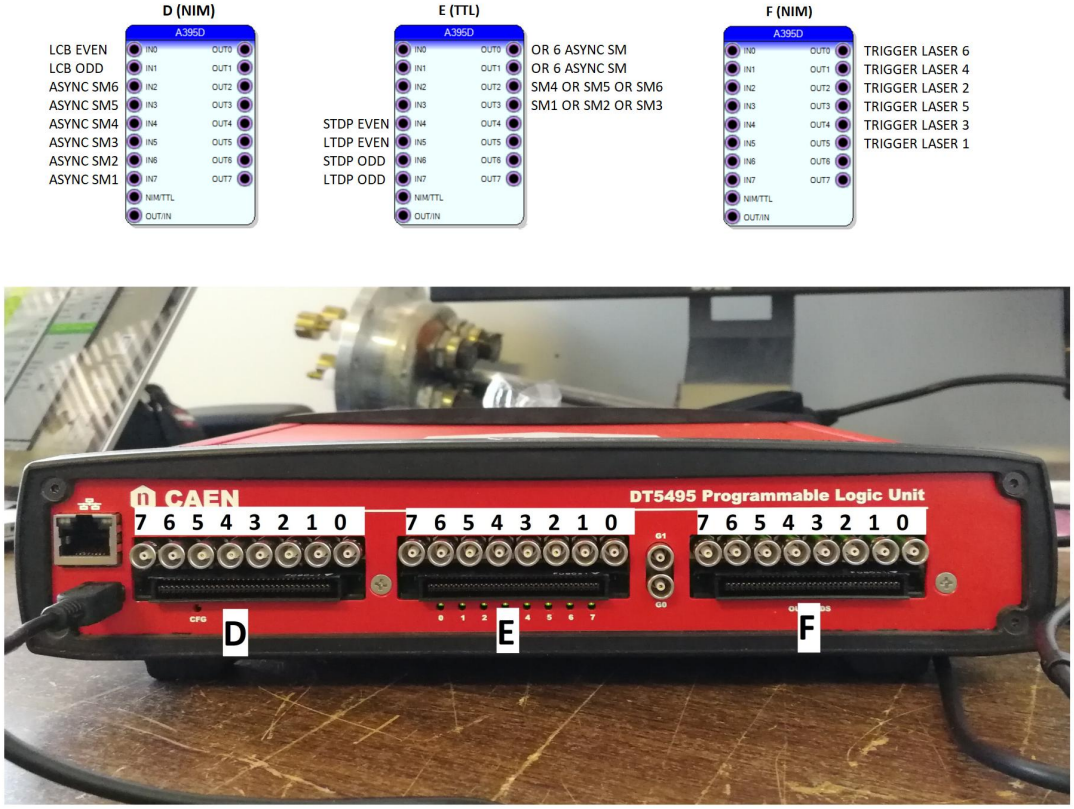

Figure 8: *DT5495: experimental setup.*

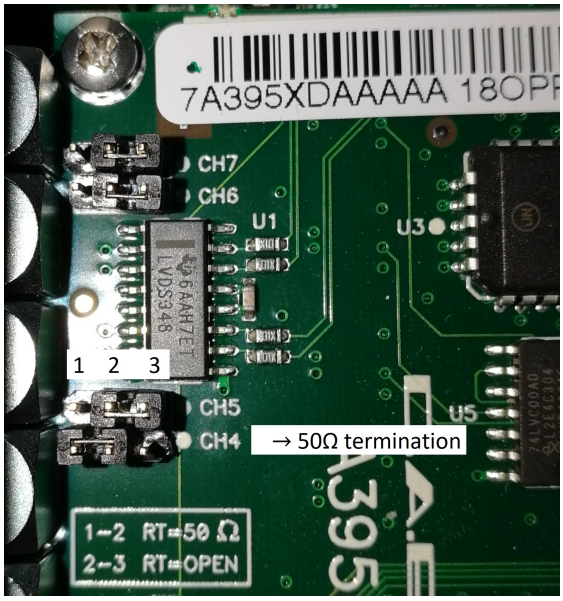

Figure 9: *Different position of jumpers.*

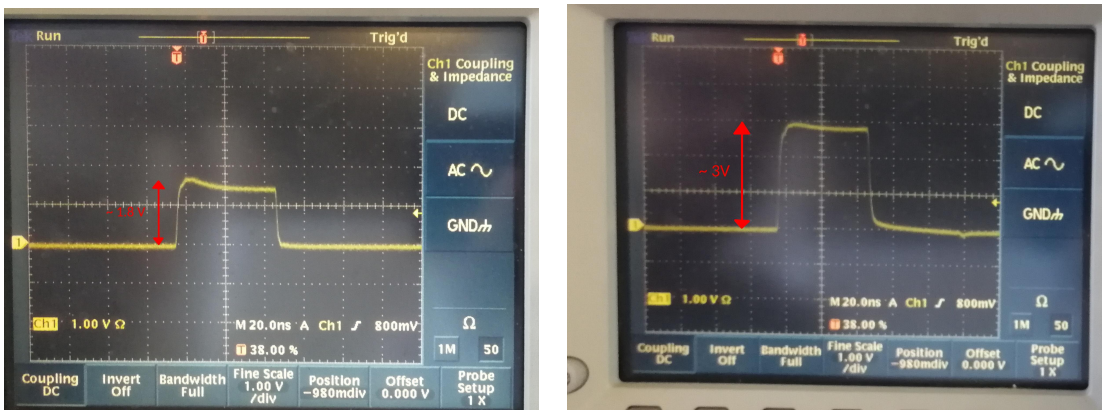

(a) *TTL output signal without 50 Ω termination.* **(b)** *TTL output signal with 50 Ω termination.*

Figure 10: *TTL output signal: before and after changing the position of the jumpers.*

3. Lost Muons Studies

During their path into the g-2 storage ring some of the muons are lost mainly because of their interaction with collimators.[1] These muons are mostly lost at early times, thus distorting the standard exponential decay. The effect can be taken into account in the final ω_a fit with by including an additional factor $\Lambda(t)$ [7] [8]:

$$N(t) = N_0\, e^{-t/\tau} \Lambda(t)\, [1 - A\cos(\omega t + \varphi)] \tag{9}$$

3.1. Incorporating muon losses into the fitting function

Let define $L(t)$ as the rate at which muons are lost from the ring. $L(t)$ does not directly enter the fitting function. In fact, each muon in $L(t)$ would have eventually decayed into a positron, and it is the absence of the later decay positrons that consitutes $\Lambda(t)$ in Equation 9. We are interested in the functional form of $\Lambda(t)$, that can be determined as shown in [8] and is:

$$\Lambda(t) = 1 - K_{LM} \int_0^t L(t')\, e^{t'/\tau} dt' \tag{10}$$

where $\tau = \gamma\tau_0 = 64.4\ \mu$s is the muon lifetime and K_{LM} is an acceptance factor that can be extracted from the fit of the ω_a.

The goal of lost muons analysis is the determination of the lost muon spectrum $L(t)$ and of its exponentially weighted integral:

$$J(t) = \int_0^t L(t')\, e^{t'/\tau} dt' \tag{11}$$

3.2. Calorimeter coincidences

Muons exiting the orbit curl inside the ring and can cross two or more calorimeters (as sketched in Figure 11) without stopping or losing a significant fraction of their energy. So, to identify lost muons, we can use double, triple or quadruple coincidences between calorimeters.

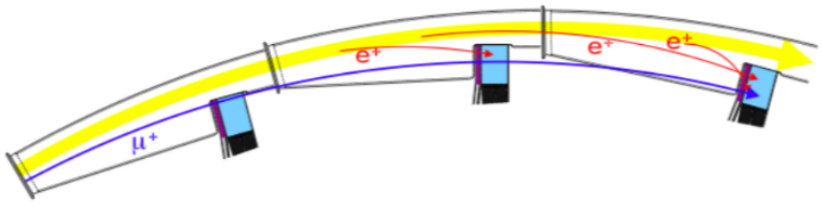

Figure 11: *Lost Muon triple coincidence event scheme. The yellow arrow represents the beam, the blue one the lost muon.*

Possible backgrounds for the lost muons measurement are the accidental coincidences

[1] Collimators are used to remove muons outside the 9 cm diameter storage region. They consist of 3mm-thick copper rings, with inner and outer radii of 4.5 cm and 5.5 cm.

of positron energy deposits and positron showers debries reaching consecutive calorimeters.
The lost muons signature is given by:

- Timing: muons travelling at the speed of light cover the ~ 1.8 m distance between consecutive calorimeters in ~ 6.2 ns.
- Cluster hit multiplicity: differently from positron showers, Minimum Ionizing Particles (MIPs), like 3.1 GeV muons, give a very localized energy deposit, involving in most cases just 1 or 2 crystals in a calorimeter.
- Energy: according to the Bethe-Bloch equation, MIPs deposit a fixed amount of energy ($\sim$ 170 MeV) in the material they crossed.
- Cluster position: muon tracks arriving from the ring should hit the first calorimeter of the coincidence in the columns close to the ring: a coincidence starting from the column furthest from the ring is most likely due to background.

4. Lost Muons preselection using real data

To familiarize with the g-2 software and with the data itself, I started the Lost Muons study analyzing data from the *60h Dataset*, intending to filter a sample of candidate lost muons using calorimeter coincidences.
I defined the lost muons using the conditions reported in Table 1. In particular, the cut on the cluster time was chosen because when the muon beam enters the magnetic ring, it is scraped to reduce muon losses from the storage ring during the measurement period [9].

Cluster time	$t > 10$ μs
Number of cluster hits	1
Clusters time difference	4.2 ns $< \Delta t <$ 8.2 ns
Cluster energy	E $<$ 300 MeV

Table 1: *Cuts used to filter calorimeter coincidences in 60h Dataset.*

Figure 12 shows the number of coincidences along the ring (only the first calorimeter in the coincidence is considered). To avoid double countings, an exclusive definition of coincidence was used, so that, for example, a coincidence is considered as double if none of its clusters belongs to a triple coincidence, and so on.
From figure 12 we see that the number of coincidences is not constant with the calorimeter number: this is because muons encounter different materials along the ring. Most of the muons are lost in the first half of the ring, since after the injection all the particles with momentum and injection angle different from the designed ones are lost. Then, the number increases right after the collimators. Muons lost due to their impact with collimators is the subject of a dedicated study I performed with MonteCarlo simulations in Sec. 5.1.

4.1. Energy and time analysis of the selected events

To check if the coincidences we are looking at belong to something that acts like a muon, a dedicated energy and time analysis was made. In particular I checked that the mean deposited energy in a single calorimeter was around 170 MeV, as expected from

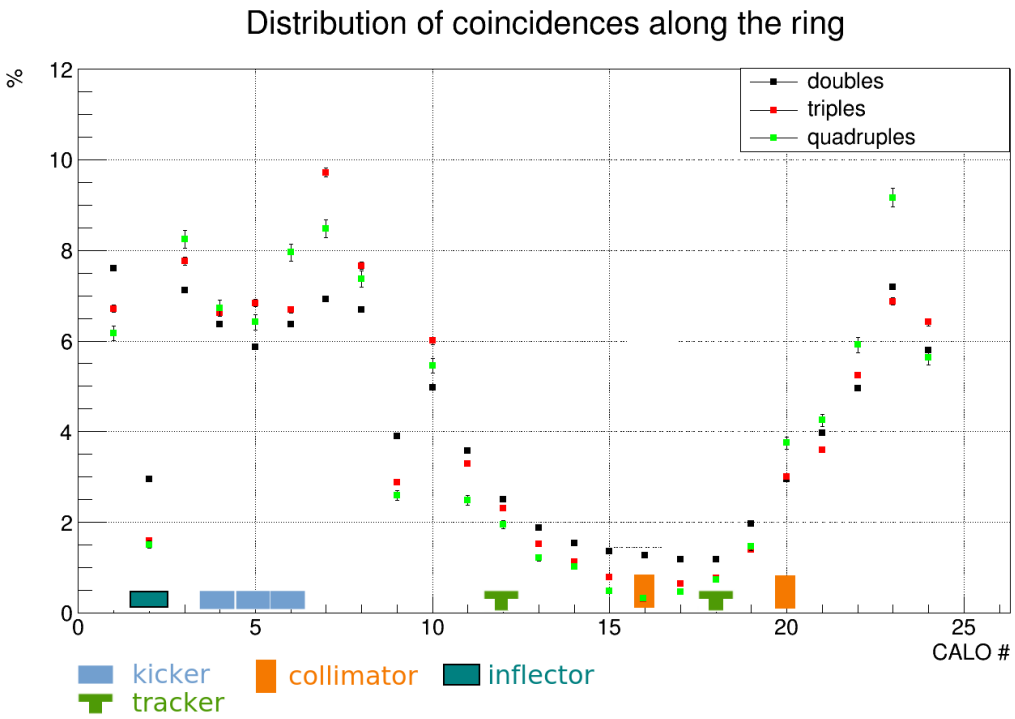

Figure 12: *Number of coincidences for each calorimeter. The distributions are normalized to 1.*

the Bethe-Bloch formula, and that the time difference between two calorimeters hits was around 6.2 ns, i.e., the time in which a muon travelling at almost the speed of light covers the distance between two adjacent calorimeters. As an example, Figures 13 and 14 show the distributions in the case of a double coincidence involving calorimeters 1 and 2 of the ring. I also checked that the muon loses almost the same amount of energy in two consecutive calorimeters, as expected for a MIP. This was done measuring the difference between the deposited energies in two adjacent calorimeters. As expected the distribution is centered at 0 MeV, as shown in Figure 15.

Similar results were obtained also for triple and quadruple coincidences and for each pair of adjacent calorimeters in a coincidence.

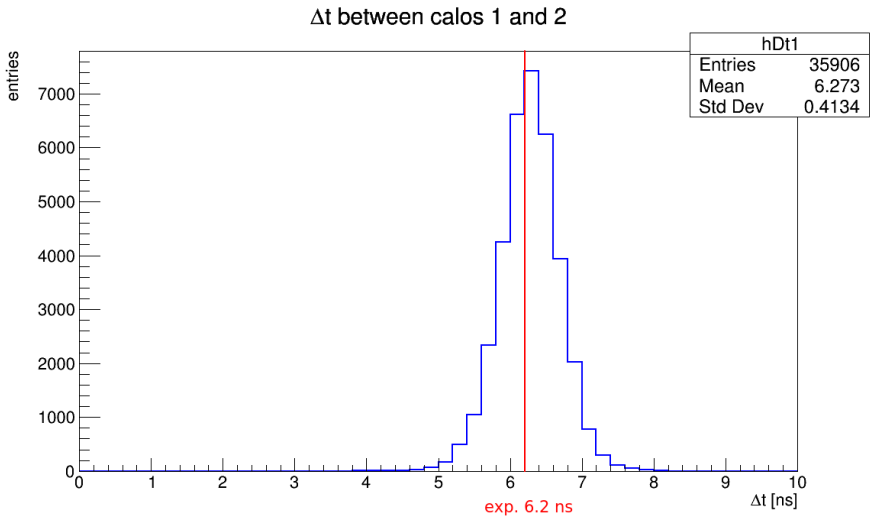

Figure 13: *Time difference distribution between calorimeters 1 and 2 hits for the selected lost muons.*

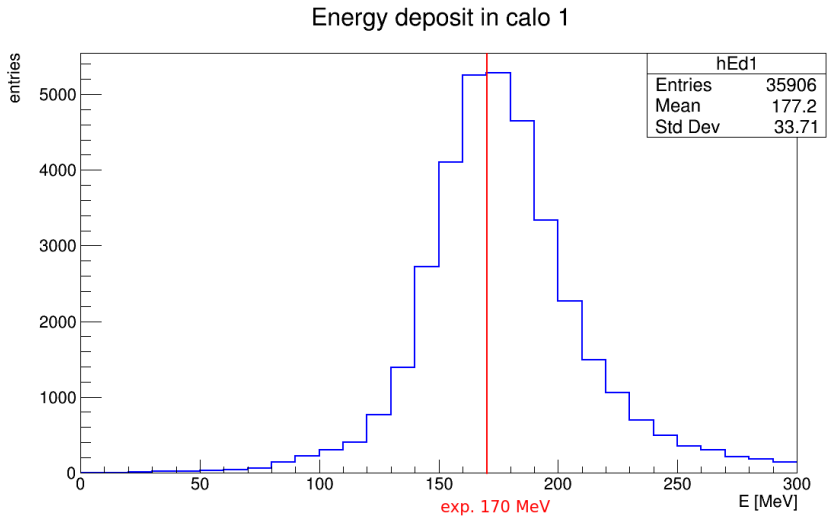

Figure 14: *Deposited energy in the first calorimeter of a double coincidence.*

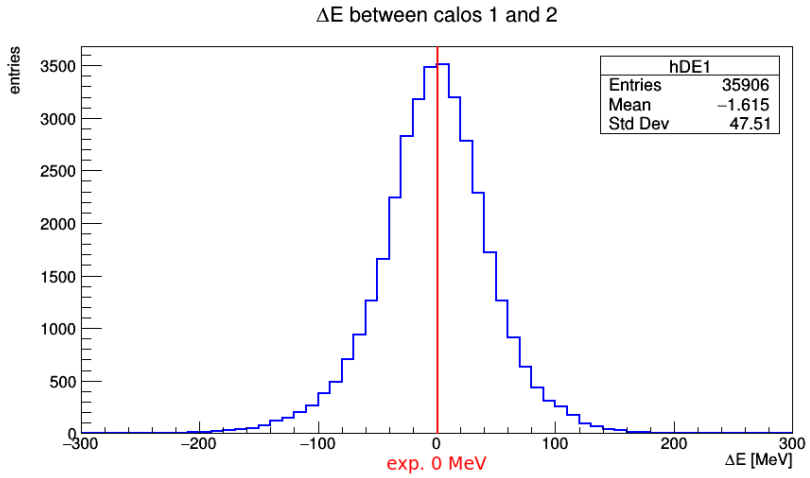

Figure 15: *Difference between the deposited energies in two adjacent calorimeters.*

5. MonteCarlo simulations analyses

One of the purposes of the Lost Muons analysis is to understand the behaviour of a muon that hits a collimator.

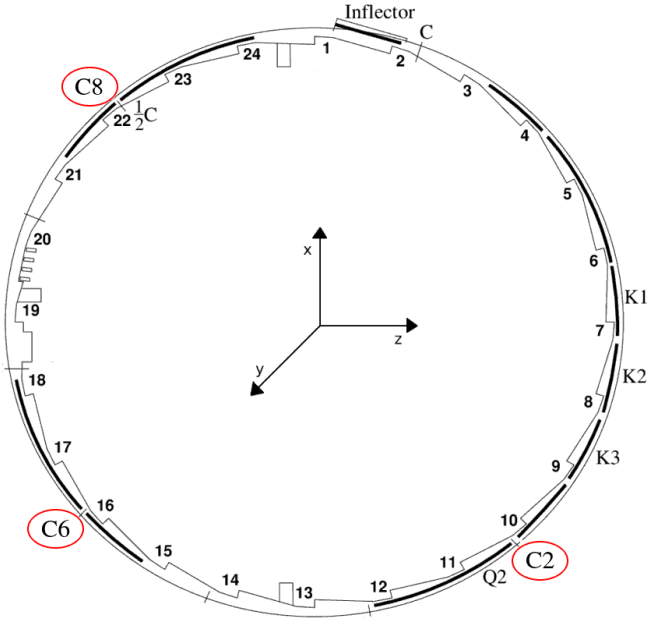

Figure 16: *The g-2 storage ring layout. The 24 numbers represent the locations of the calorimeters, while C2, C6 and C8 represent the location of the collimators.*

For these studies we define a muon "lost" as soon as it exits the storage region. The radius of the g-2 ring, i.e. the distance from the center of the ring to the center of the storage region, is $r_{Magic} = 7112$ mm, while the radius of the storage region (Fig. 17) is $r_{storage} = 45$ mm.

Figure 17: *Inside view of the g-2 ring: storage region.*

Defining:

$$r = \sqrt{x^2 + z^2} - r_{Magic} \tag{12}$$

where x and z are the coordinates on the ring plane (as Figure 16 shows), we say that a muon is lost if:

$$\sqrt{r^2 + y^2} > r_{storage} \tag{13}$$

We are interested to the lost muons that satisfy Eq. 13 and hit a collimator. In particular we would like to study when and where a collimator is hit, the momentum of muons that hit a collimator, and also if after hitting a collimator a muon hits two or more calorimeters, and if so, how much energy it deposits in it. It is important to perform these studies in MonteCarlo events since this could help us to improve the recognition of lost muons in the real data.

5.1. "BEAM_GUN_WITH_COLLIMATOR" SIMULATION

I started analyzing an *ad hoc* MonteCarlo, where a single muon beam is simulated and sent on purpose on a collimator. This first step was preferred in order to implement and test a code running on something with a higher statistics, so as to decrease the execution time.
In this simulation, all muons are generated with the magic momentum, and they all hit C8 always at the same time ($\simeq$ 80 ns) and always in the same position.

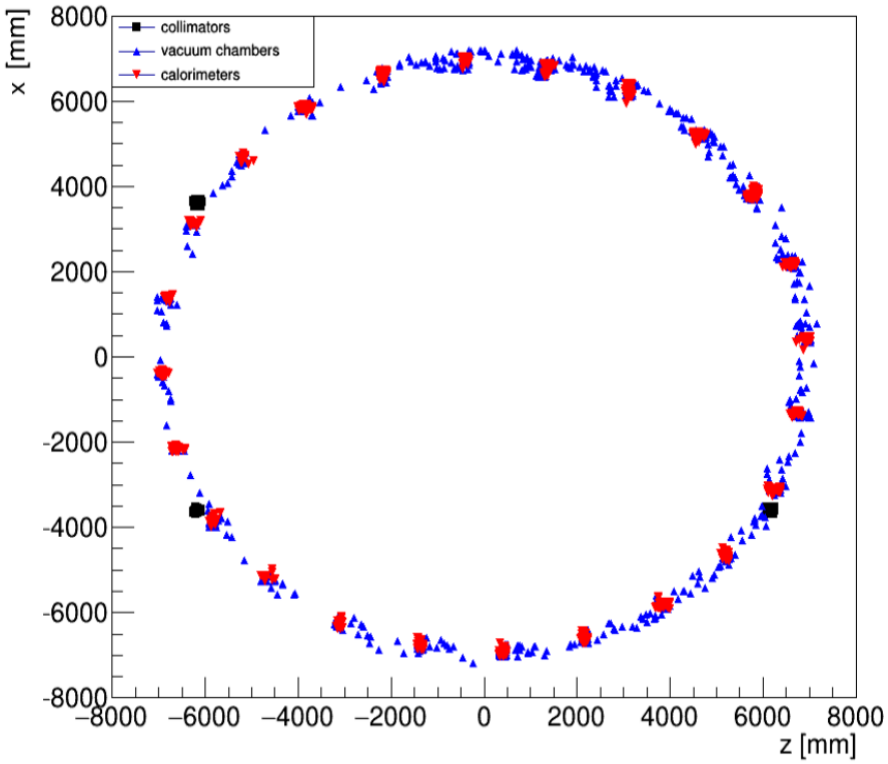

Figure 18: *Upper view of the g-2 ring, showing what lost muons hit outside the storage region.*

After the muon hits a collimator, it can either decay or it can continue its path hitting other material, like calorimeters and vacuum chambers. Figure 18 represents an upper view of the g-2 ring, showing the trajectory of lost muons outside the storage region,

in particular when they hit a collimator (in black), a vacuum chamber (in blue) or a calorimeter (in red).
Collimators can be hit more than one time before the muon exits the storage ring: sometimes after hitting C8, muons interact with C2 and C6 as shown in Fig. 19a and 19b and in 4% of the cases they hit C8 again as shown in Fig. 19c. In this type of plots, r is calculated as in Eq. 12, while y is the vertical coordinate.

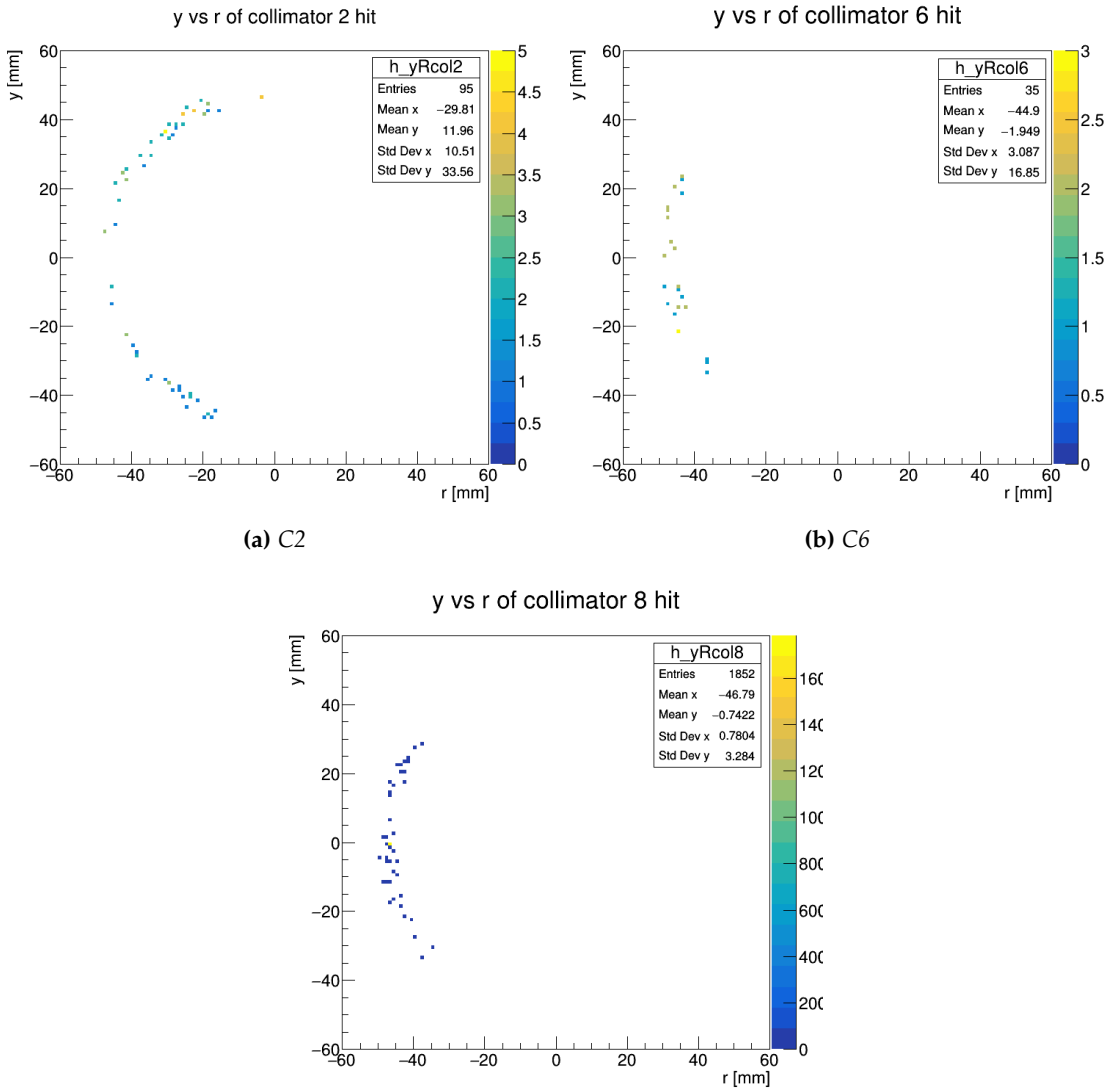

(a) *C2*

(b) *C6*

(c) *C8*

Figure 19: *y and r of where C2, C6 and C8 are hit by a lost muon. (beam_gun_with_collimator simulation)*

The fraction of the momentum lost by the muons hitting a collimator is about 1%, as shown in Figure 20.
After muons exit the storage region they will act as MIPs and they can hit more than one calorimeter. In Figure 21a is shown the normalized distribution of the number of calorimeters hit by lost muons in a multiple coincidence. This distribution is interesting because in real data (see Sec. 3.2) lost muons are selected looking at triple

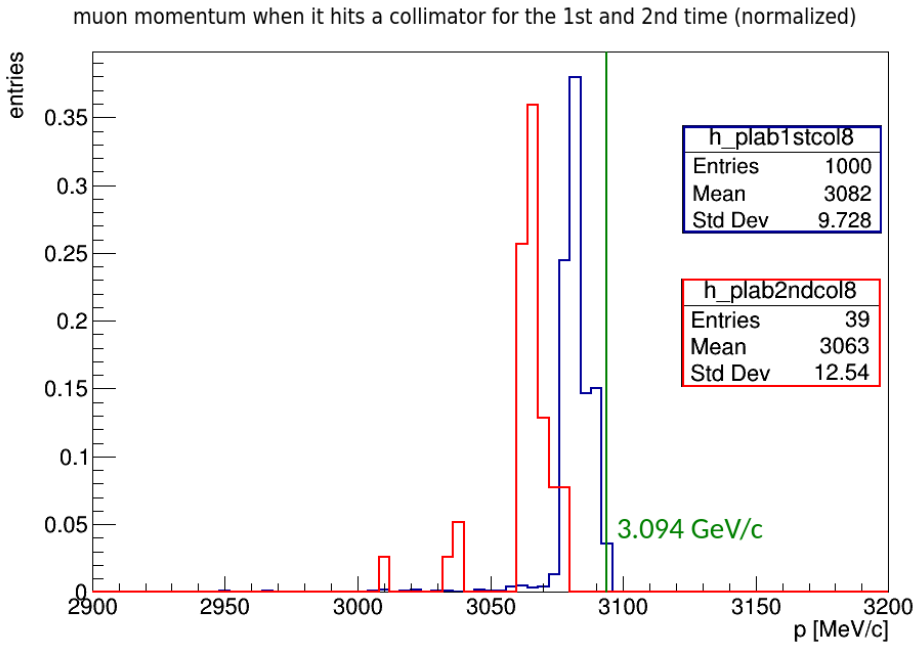

Figure 20: *Muons momentum when they hit C8 for the first time (blue line) and for the second time (red line). (beam_gun_with_collimator simulation)*

coincidences (with particular cuts on energy and cluster time), and in this particular case only $\sim 10\%$ of lost muons make a triple coincidence.
Let's define *REAL+SIG muons*, in our MonteCarlo simulation, as those muons that hit three adjacent calorimeters in a row.
Just as a first example of application, we can see how many collimators the *REAL+SIG muons* hit before making a triple coincidence (Figure 21b). Of course, in this particular simulation, there is always at least one collimator hit, but we see that sometimes, before the lost muon makes a triple coincidence, it hits even two collimators.
This and other aspects will be studied and discussed in Sec. 5.2, when there will be more statistics.

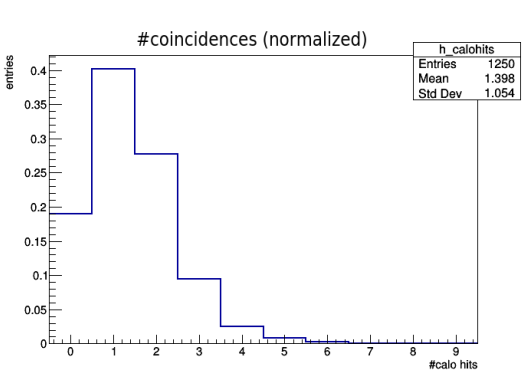

(a) *Distribution of the number of calorimeters hit by a lost muon.*

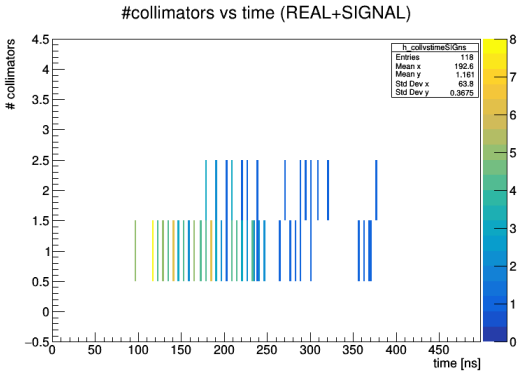

(b) *Number of collimator hits by REAL+SIG muons*

Figure 21: *(beam_gun_with_collimator simulation)*

5.2. Run1 simulation

The *beam_gun_with_collimator* simulation was useful to study the features of the lost muons that hit a collimator, but to properly characterize the lost muons I analyzed the official MonteCarlo simulation of the *Run1* that simulates typical events we would see in real data.
The MC sample contained 6.7×10^7 lost muons, a good amount of statistics to study a lot more interesting features of lost muons events.
During Run1 datataking only two collimators were used, thus in this case lost muons hit collimator C6 and C8. In particular, when a lost muon hits for the second time a collimator, it does it more uniformly, as Figures 22b and 22d show.

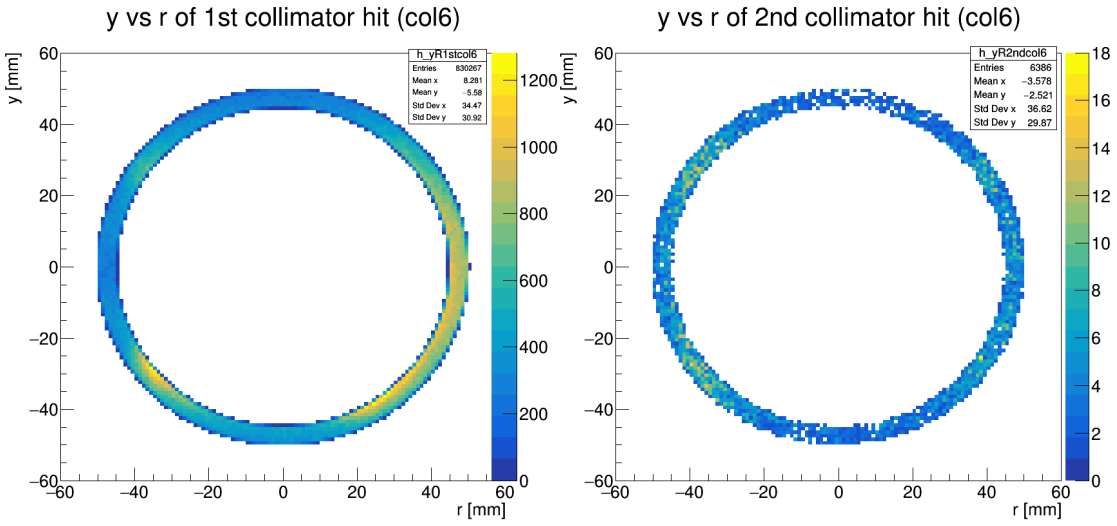

(a) *y and r of C6 when it is hit for the first time.*

(b) *y and r of C6 when it is hit for the second time.*

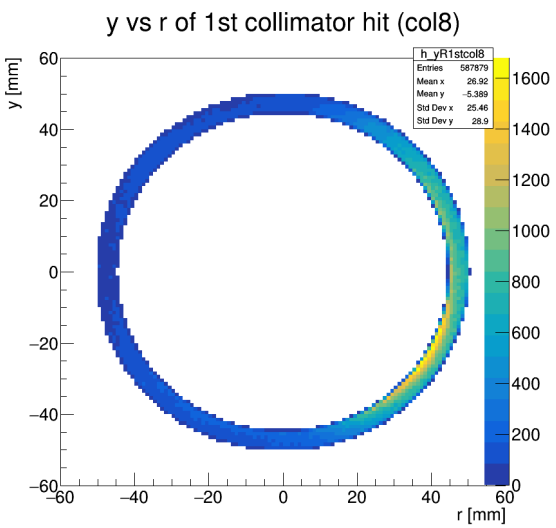

(c) *y and r of C8 when it is hit for the first time.*

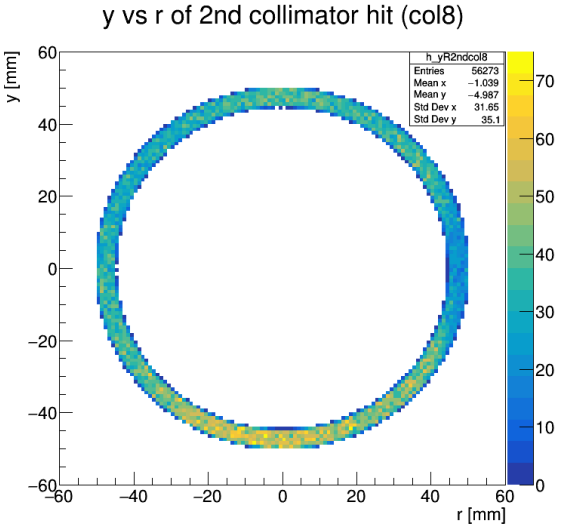

(d) *y and r of C8 when it is hit for the second time.*

Figure 22: *y and r of where C6 and C8 are hit by a lost muon for the 1st and 2nd time. (Run1 simulation)*

As in the *beam_gun_with_collimator* simulation, also in this case the fraction of the momentum lost by the muons hitting a collimator is about 1%, as shown in Figure 23.

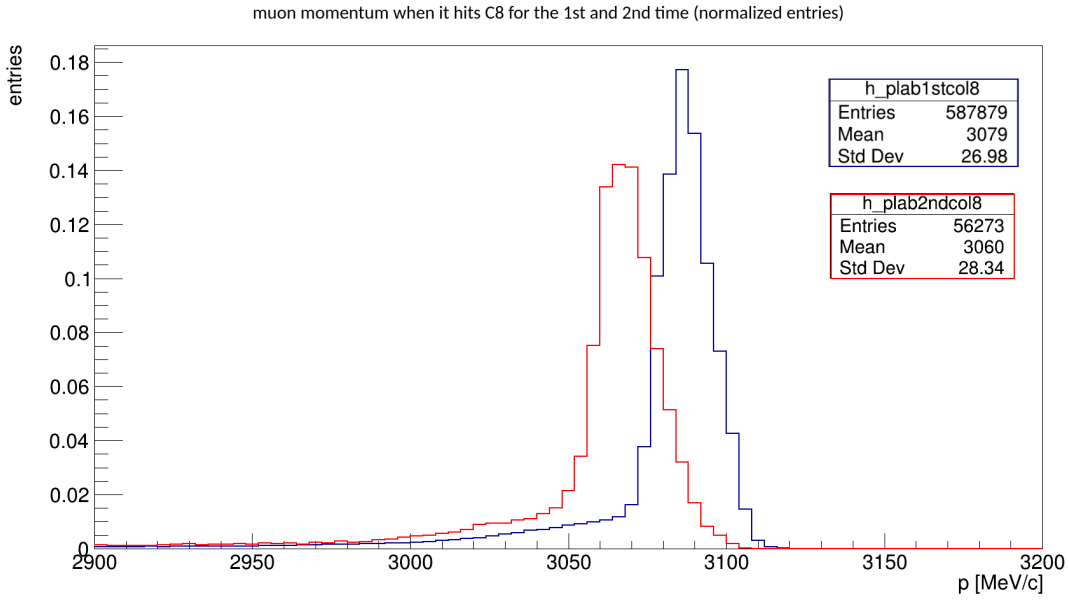

Figure 23: *Muons momentum when they hit C8 for the first time (blue line) and for the second time (red line). (Run1 simulation)*

Since this time it is not simulated a mono-energetic single muon, but a muon beam with a spread on the initial momentum, the distributions have a larger standard deviation from the center value. It can also be noticed a lower energy tail in both distributions: they are due to the those muons that turn several times around the ring before hitting a collimator, and they lose energy hitting other parts of the ring, like quadrupole plates.

Figure 24 shows the time-distance between two collimator hits as a function of the second collimator hit. In some cases, a lost muon travels even $\sim$ 400 ring turns (!) before hitting a collimator for the second time.

Figure 25 shows the normalized to unit distribution of the number of calorimeters hit by lost muons in a multiple coincidence. About 14% of lost muons make a triple coincidence.

We defined *REAL+SIG muons* lost muons that make a triple calorimeter coincidences. Since in this simulation the muon beam is not sent on purpose on a collimator, now it is interesting to see how many collimators a lost muon hits before making a triple coincidence.
This is shown in Figure 26a. A zoom on the first microsecond is reported in Figure 26b.

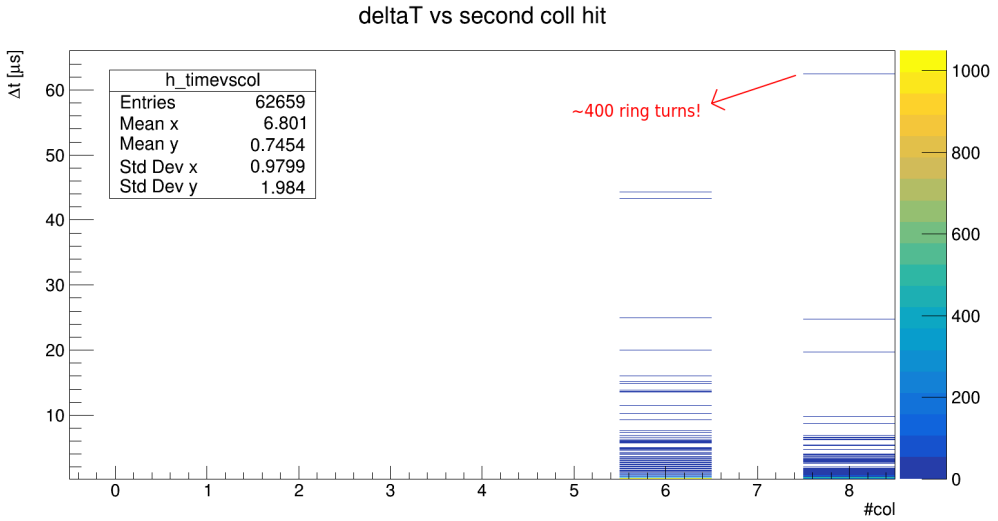

Figure 24: *Time-distance between two collimator hits as a function of the second collimator hit. (Run1 simulation)*

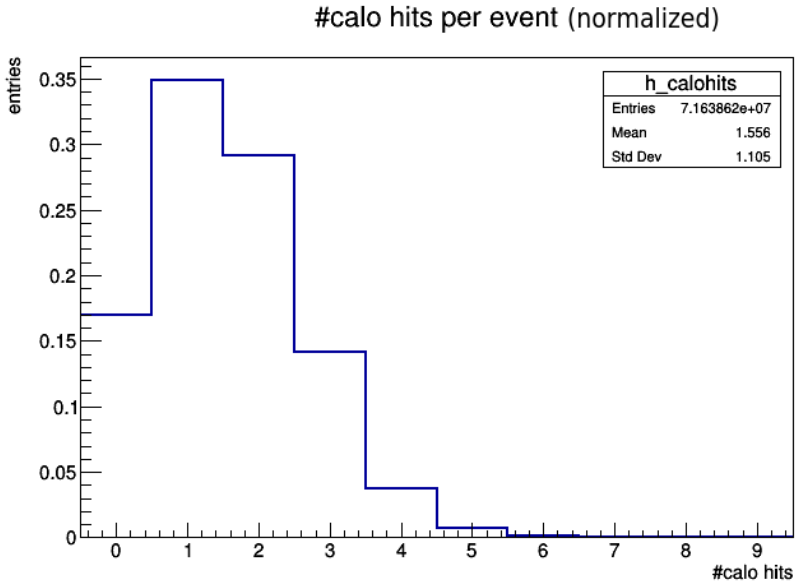

Figure 25: *Distribution of the number of calorimeters hit by a lost muon. (Run1 simulation)*

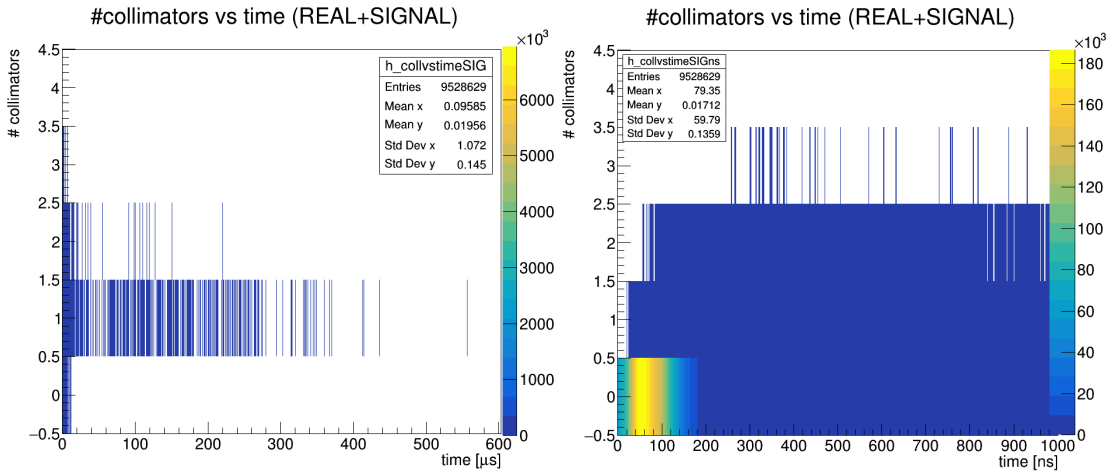

(a) **(b)**

Figure 26: *Number of collimators hit by REAL+SIG muons as a function of time. (Run1 simulation)*

The most part of the lost muons exit the ring at early times without hitting a collimator. This time window is the *scraping phase* which, as discussed previously, for real data we do not consider. After 10 μs almost all lost muons that made a triple coincidence have previously hit a collimator. Of all the lost muons that make a triple calorimeter coincidence only 0.007% survives after the 10 μs selection cut. This number is even smaller if we compare it with the total number of lost muons: considering that only in the 14% of the cases a lost muon makes a triple coincidence, the fraction of lost muons that we see cutting at 10 μs and looking at triple coincidences becomes 0.0005%. To properly study these lost muons we need more statistics.

Figure 27a shows the distribution of Δt_{lost} defined as the time-distance between when a first calorimeter of a triple coincidence is hit and when the muon hits a collimator for the first time. A zoom on the first microsecond is shown in Figure 27b.
Most of the *REAL+SIG muons* that hit a collimator make a triple calorimeter coincidence after $\sim$ 100 ns. After few hundreds of nanoseconds, the distribution in Figure 27a decreases exponentially (notice the logarithmic scale on the y axis).

Figure 28 shows the total energy deposited E_{dep} in all the calorimeters of a coincidence. Reasonably, E_{dep} increases linearly with the number of calorimeters hit. In Figure 29 there is a better view of how much energy is deposited in the crystals.
In the simulation, lost muons deposit about 120 MeV in each calorimeter they cross. This is lower than the 170 MeV expected by the Bethe-Bloch Formula. The discrepancy is acceptable for these purposes, and is a consequence of runtime optimizations.

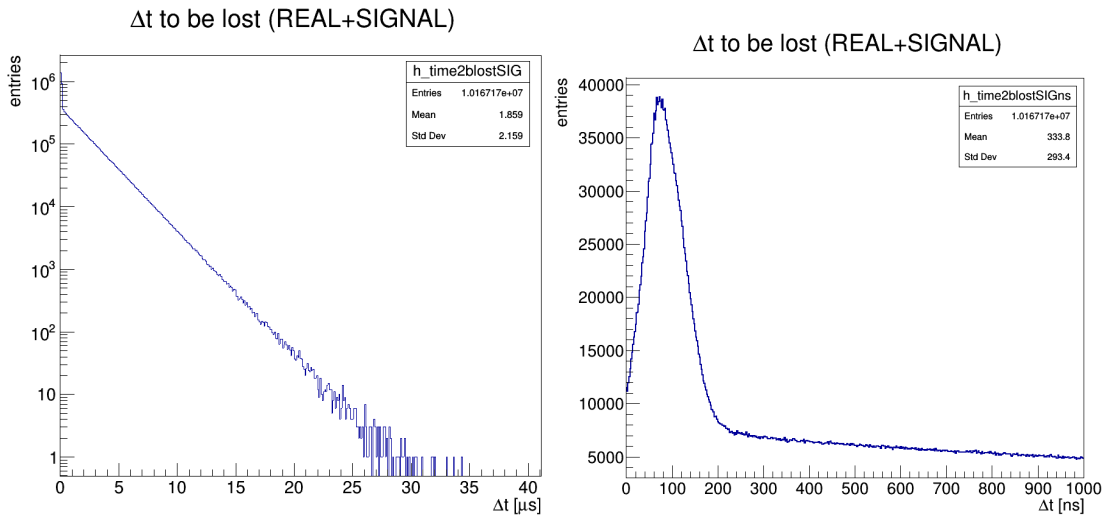

(a) **(b)**

Figure 27: *Distribution of the time-distance between when a first calorimeter of a triple coincidence is hit and when the muon hits a collimator for the first time. (Run1 simulation)*

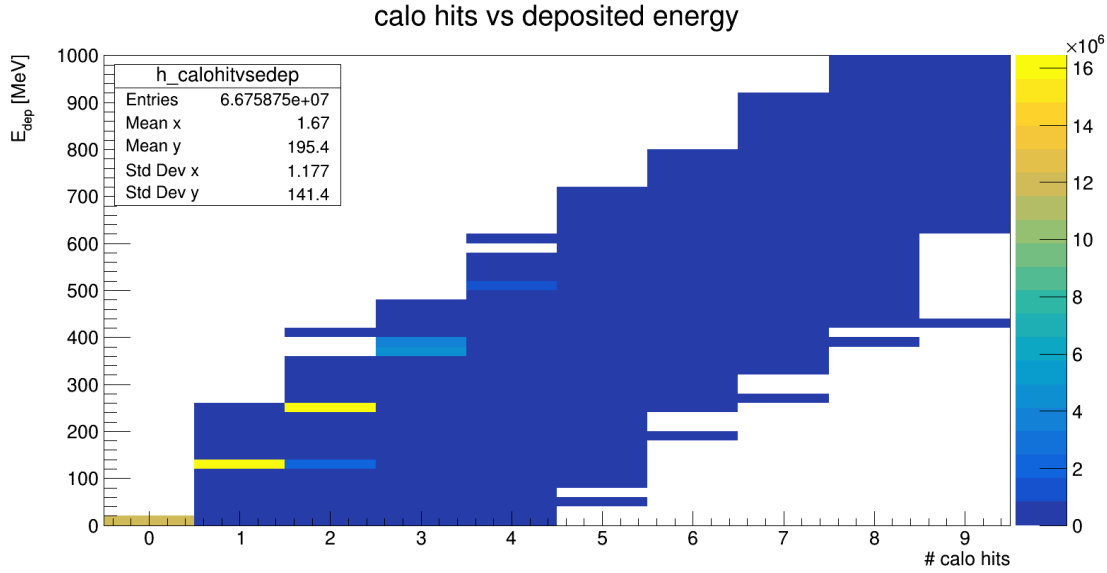

Figure 28: *Energy deposited in all the calorimeters of a coincidence as a function of the total number of calorimeters hit. (Run1 simulation)*

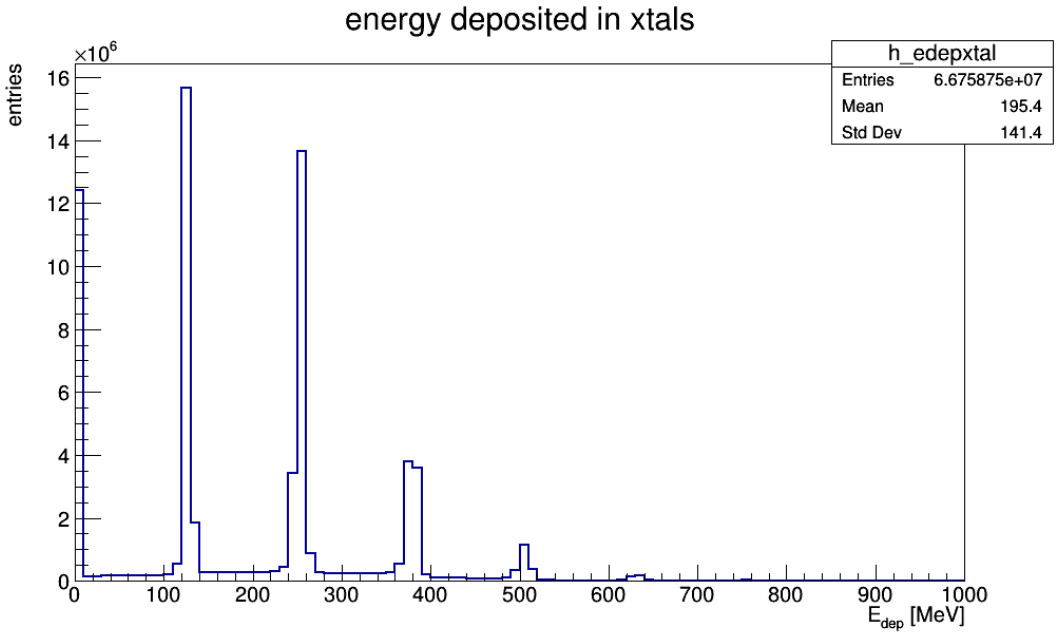

Figure 29: *Distribution of the energy deposited in the crystals. (Run1 simulation)*

6. Conclusions

These two months have been an extraordinary experience for me. I learned a lot of things, from the notions of physics to hardware and software techniques. I also improved my programming skills a lot.
I hope to have the opportunity to continue working on the analysis of Lost Muons as many questions are still open. In particular, I would like to use the results obtained to make a more accurate comparison between the data and MonteCarlo.

Finally, I would like to thank prof. Incagli and Anna for always being available to help me, for all the things they taught me and above all for the patience they had with me.

References

[1] Donald H. Perkins, *Introduction to High Energy Physics*

[2] W. Gohn, *The Muon g-2 experiment at Fermilab* https://arxiv.org/abs/1611.04964

[3] A. Keshavarzi, *The Muon g-2 experiment at Fermilab* https://arxiv.org/pdf/1905.00497.pdf

[4] S. Ganguly, J. D. Crnkovic, W. M. Morse, D. Stratakis, *Lost Muon Study for the g-2 experiment at Fermilab*

[5] Anastasi et al., *The laser calibration system of the Muon g-2 experiment at Fermilab*

[6] Anastasi et al., *The laser control of the muon g-2 experiment at Fermilab*

[7] S. Di Falco, A. Driutti, A. Gioiosa, M. Sorbara, *Lost Muons Correction*

[8] Chris C. Polly, *A measurement of the anomalous magnetic moment of the negative muon to 0.7 ppm*

[9] On Kim et al., *A method to reduce the coherent betatron oscillations in a muon g-2 storage ring experiment using RF fields* https://arxiv.org/pdf/1902.02959.pdf

[10] S. Ganguly, *Muon g-2: Measuring the Muon Magnetic Anomaly to High Precision (52nd Annual Fermilab Users Meeting)*